Applied Thermal Engineering 173 (2020) 115219

Contents lists available at ScienceDirect

Applied Thermal Engineering

journal homepage: www.elsevier.com/locate/apthermeng

Lab-scale sorption chiller comparison of FAM-Z02 coating and pellets

C. McCague, W. Huttema, A. Fradin, M. Bahrami*

Laboratory for Alternative Energy Conversion (LAEC), School of Mechatronic Systems Engineering, Simon Fraser University, 250-13450 102 Avenue, Surrey, BC V3T 0A3, Canada

HIGHLIGHTS

- Lab-scale sorption chiller tests of SAPO-34 coated heat exchangers.
- Specific cooling power of 456 W/kg (90 kW/m^3) for 10 min cycles.
- Comparison of material properties of SAPO-34 powder, coatings and pellets.

ARTICLE INFO

Keywords:
Sorption chiller
ASQOA FAM-Z02
Specific cooling power
Coefficient of performance

ABSTRACT

Water adsorbent AQSOA™ FAM-Z02 (Z02) coatings and pellets were evaluated in our custom-built lab-scale sorption chiller with two adsorber beds. Two finned-tube heat exchangers (HEX) (4.08 L) were coated with Z02 by Mitsubishi Plastics and compared with two other HEX that were packed with Z02 pellets. When tested with 15, 30, 30 and 90 °C operating temperatures for the evaporator, condenser, adsorption and desorption, and 5–30 min cycle times, the sorption chiller had a peak volumetric specific cooling power of 90 ± 5 kW/m^3 with Z02-coated HEX compared to 59 ± 2 kW/m^3 for HEX packed with Z02 pellets. The specific cooling power (SCP) and coefficient of performance (COP) were greater for Z02 coatings compared to pellets.

1. Introduction

Silicoaluminophosphate SAPO-34 zeolite was developed and commercialized as AQSOA™ FAM-Z02 by Mitsubishi Plastics Inc. as a water adsorbent for use in desiccant wheels and adsorption chillers operating with low regeneration temperatures [1]. Z02 has an S-shaped isotherm and a $\Delta w \cong 0.21$ g/g (H_2O/sorbent) under 15, 30, 30, 90 °C sorption chiller operation cycle temperatures (evaporator, condenser, adsorption and desorption, respectively). Freni et al. [2] used a mathematical model to evaluate the sorption cycle performance of numerous adsorbent/adsorptive working pairs and concluded that, amongst water sorbents for air conditioning applications, Z02 and salt-silica gel composites had the highest potential coefficient of performance (COP) and specific cooling power (SCP).

The dynamics of water ad-/desorption by Z02 loose grains were studied by Girnik et al. through volumetric large temperature jump (V-LTJ) tests on monolayers and multilayers of Z02 pellets [3,4]. They found a "grain size insensitive regime" for uptake when comparing samples with equal values for the ratio of heat transfer surface area to adsorbent mass (S/m) from 0.44 to 1.75 m^2/kg (e.g. S/m = 1.75 m^2/kg for two layers of 0.4–0.5 mm grains or four layers of 0.2–0.25 mm grains) and found that the cycle power increased linearly with increasing S/m [3]. Temperature-step adsorption and desorption dynamics tests on 70–90 g of Z02 packed into small heat exchangers (~0.2 m^2) with three designs, each with a compactness of ~1100 m^2/m^3, were conducted by Santamaria et al. [5]. The dynamic behaviour for different Z02 grain sizes was found to be a function of S/m for grain sizes less than 1 mm, and cooling powers up to 2.3 kW per kilogram of sorbent were reported, 6–8 times greater that the cooling powers achieved in tests of larger prototypes [5].

To determine the relative importance of heat and mass transport impedances, J. Ammann et al. conducted isochoric temperature swing tests on coatings of SAPO-34 with 5 wt% binder and found that mass transport limited the sorption dynamics for all coating thicknesses tested (0.06–0.46 mm) [6].They found that the water adsorption rate increased by up to two times when longitudinal channels were introduced into coating layers in a structure that improved mass transfer while maintaining same adsorbent mass to unit area [7]. In an earlier study of silica gel spheres on a metallic substrate, J. Ammann et al. found the sorption rate was dominated by heat transport impedances, although the mass transport impedance for 1.8–2.0 mm sized beads also contributed significantly to total transport impedance [8]. The effects of

* Corresponding author.
E-mail address: mbahrami@sfu.ca (M. Bahrami).

https://doi.org/10.1016/j.applthermaleng.2020.115219
Received 15 June 2019; Received in revised form 1 March 2020; Accepted 17 March 2020
Available online 19 March 2020
1359-4311/

adsorbent intra-particle mass diffusion, interparticle flow resistance and thermal transport have also been theoretically studied with respect to optimizing heat exchanger geometry by Mitra et al. [9].

Accelerated aging tests performed by Freni et al. confirmed the hygrothermal stability of Z02 coatings prepared by Mitsubishi Plastics Inc. and SAPO-34 coatings that they prepared [10]. In further experiments, Freni et al. compared aluminium finned flat tube heat exchangers (HEX) (510 g) that were coated with SAPO-34 (0.1 mm thick, 84 g) to HEX that were filled with granular SAPO-34 (0.6–0.7 mm grains, 260 g) using a lab-scale single bed sorption chiller under 15/28/28/90 °C operating temperatures [11]. For 5 min cycles, the coated HEX had a SCP of 675 W/kg and volumetric SCP of 93 kW/m^3, while the SCP of the HEX filled with granular Z02 (0.6–0.7 mm) was 498 W/kg (212 kW/m^3). The cooling COP was 0.24 for the coated HEX compared to 0.4 for the granular HEX with its substantially higher sorbent/HEX ratio. In a subsequent study, heat exchangers (HEX) coated with Z02 and then filled with granular microporous silica gel were tested in a three adsorber bed sorption chiller. The SCP for was 508 W/kg and 658 W/kg for operating conditions of 15/28/28/90 °C and 15/25/25/90 °C, respectively. However, the VSCP increased significantly up to 286.4 kW/m^3 (by adsorber volume), and a VCP$_{chiller}$ of 9.8 kW/m^3 calculated considering the volume of the system [12].

Dawoud tested Z02 coatings deposited by Mitsubishi Plastics on small substrates and HEX. For small samples, as the coating thickness was increased from 0.2 to 0.5 mm, the adsorption rate decreased by 47%. However, for Z02 coatings on extruded finned-tube and finned-plate HEX the adsorption rates were substantially lower [13].

SAPO-34 was directly crystallized on a novel aluminium fiber flat tube HEX (3.3 kg adsorbent on 8.5 kg HEX) by Wittstadt et al. and tested in a single vacuum chamber that also contained an evaporator/condenser. For 18/27/85 °C nominal operating conditions, the sorber had a module volume specific cooling power of 82 kW/m^3 and a COP of 0.4 for cooling [14]. Calabrese et al. recently reviewed adsorbers coated with SAPO-34 based zeolite for adsorption heat pumps, identifying issues and presenting new coating formulations with improved mechanical and thermal properties [15].

During initial tests of our sorption chiller with finned-tube HEX packed with 2 mm diameter Z02 grains, reported by Sharafian et al. [16], the highest SCP (119 W/kg adsorbent) was observed when the adsorbent loaded into each of the two HEX was reduced from 1.9 to 0.5 kg. At that time, the system performance was limited by the heat transfer rate in the evaporator and pressure drops in the piping and valves between the evaporator and the sorber beds in our testbed [16]. In the present study, an improved sorption chiller testbed was used to compare the performance of Z02 pellets and coatings. Upgrades made to the sorption chiller testbed include: (i) installation of four-way valves for faster adsorption to desorption temperature switches between the two sorber beds, (ii) larger diameter pipes and gate valves between the evaporator and sorber beds, and iii) a more powerful capillary-assisted low-pressure evaporator. The improvements result in higher system SCP and greater ability to compare sorbent and sorber bed performance.

2. Experiments

2.1. Material characterization

Water adsorbent silicoaluminophosphate powder (AQSOA™ FAM-Z02 powder, Lot # ZZ114913) and 1.4–2.4 mm pellets containing silicoaluminophosphate powder and silicon dioxide-based binder (6–17 wt%) (AQSOA™ FAM-Z02 pellets, Lot # ZA115401) were acquired from Mitsubishi Plastics Inc. Two finned tube heat exchangers (engine oil cooler, model #1268, Hayden Automotive) and an aluminium plate were coated with a silicoaluminophosphate powder and silicon dioxide-based binder (10 wt%) by Mistubishi Plastics using their proprietary method and the average coating thickness was 0.33 mm. The Z02 coating samples were flaked from the aluminium plate without scratching the substrate or any metal inclusions in the sample.

Water isotherms and isobars were collected on samples of Z02 powder, coating, and spherical pellets (5 pellets, average diameter 1.90 ± 0.08 mm measured by optical microscopy) using a thermogravimetric vapor sorption analyser (TGA) with active pressure control (IGA-002, Hiden Isochema). Water uptake, w, is reported as

$$w = \frac{mass\ \ H_2O}{mass\ \ dry\ \ sorbent} \tag{1}$$

High resolution isotherms (0.3–0.5 mbar steps) were collected at seven temperatures ranging from 5 °C to 80 °C. From this data set, isosters for water uptakes ranging from 0.11 to 0.32 where plotted, ln (P_{H2O}) vs $1/T$, and the isosteric heat of water sorption for the pellets was determined as a function of water content from the slopes of the linear plots using the Clausius-Claperyon equation

$$\ln(P_{H2O}) = \frac{-\Delta H_{is}}{R}\left(\frac{1}{T}\right) + C$$

where ΔH_{is} is the isosteric heat of adsorption (J/mol), R is the universal gas constant (8.31446 J K^{-1} mol^{-1}), T is the absolute temperature (K), and C is a constant.

Nitrogen adsorption isotherms were measured using an Autosorb iQ-MP (Quantochrome Instruments) to determine the porous properties of the Z02 pellets and coating.

2.2. System description

The lab-scale sorption chiller is shown in Fig. 1. The two sorber beds were connected to two heating/cooling (H/C) circulators using two four-way valves for automated cycling from adsorption to desorption temperatures. The HEX fins coated with Z02 and packed with Z02 pellets are shown in Fig. 2. The sorber bed specifications and operating conditions are given in Table 1. Two additional heating/cooling circulators controlled the temperature of the condenser and the custom-built capillary-assisted low-pressure evaporator (CALPE). The evaporator features a serpentine HEX with 12 tubes, each 35.5 cm long and 1.9 cm in diameter, with 1.47 mm fin height, 0.64 mm fin spacing and an inner spiral groove (Turbo Chil-40 FPI, Wolverine Tube Inc.). The inner and outer surface areas of the evaporator are 0.051 m^2/m and 0.263 m^2/m. The overall heat transfer coefficient measured by our custom-built apparatus for evaluating cooling power [17,18] was 1760 W/(m^2·K). When operated at 2.5 L/min flow rate, the evaporator has a cooling capacity of 960 W.

Vapor flow was controlled by a check valve (cracking pressure < 0.25 kPa) between each sorber bed and the condenser, and by a 50 mm gate valve between each sorber bed and the evaporator. Three positive displacement flow meters (FLOMEC, OM015S001-222) with accuracy of 0.5%, four pressure sensors (Omega, PX309-005AI) and 0.4 kPa accuracy, and ten T thermocouples (Omega, 5SRTC-TT-T-36-36) with ± 1.0 °C accuracy and two RTD thermocouples (Omega, PR-13) with ± 0.15 °C accuracy were used for detailed monitoring of the cycle. The sorber bed specifications and operating conditions are listed in Table 1.

The total heat transfer measured at the evaporator per cycle, Q$_{evap}$ (J), is calculated as

$$Q_{evap} = \int_0^{\tau} \dot{m} c_p (T_{in} - T_{out}) dt \tag{2}$$

where the mass flow rate of cold water, $\dot{m}$, is 2.5 L/min, and the specific heat for water, c_p, is 4.18 kJ/kg. The coefficient of performance (COP), specific cooling power (SCP) and volumetric specific cooling power (VSCP) are calculated as follows

$$COP = Q_{evap}/Q_{heat} \tag{3}$$

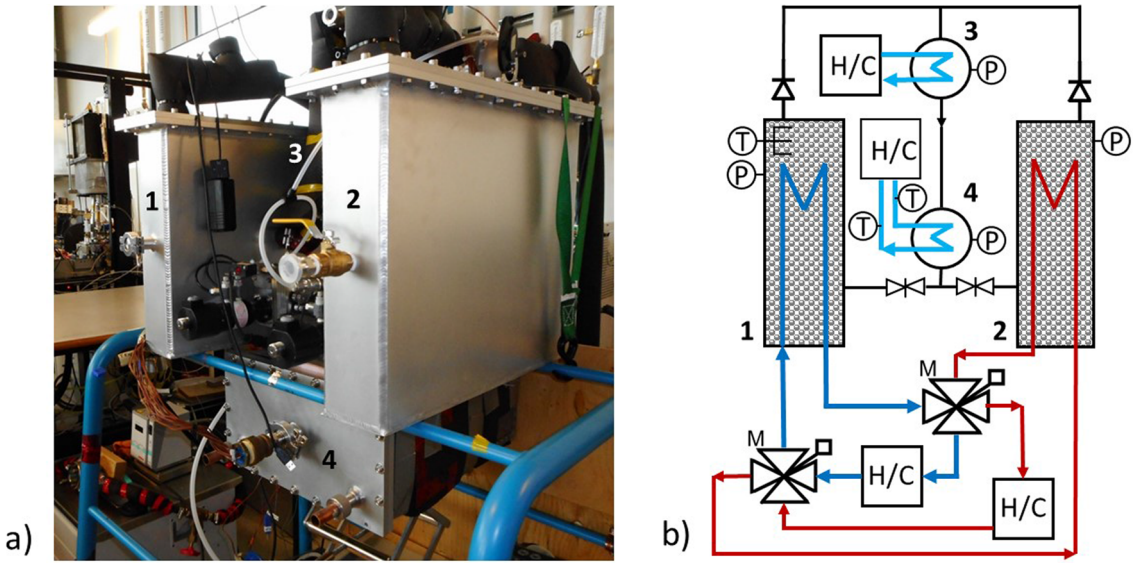

Fig. 1. (a) Photo and (b) schematic of the lab-scale sorption chiller with two sorber beds (1,2), condenser (3), capillary-assisted low-pressure evaporator (CALPE) evaporator (4), valves, sensors and heating/cooling (H/C) circulators.

$$SCP = Q_{evap}/(m_{ads} \cdot t_{cycle}) \quad (4)$$

$$VSCP = Q_{evap}/(V_{ads} \cdot t_{cycle}) \quad (5)$$

The water uptake of the adsorbent as a function of time can be calculated from the heat transfer at the evaporator. Dimensionless uptake, $X(t)$, can be described as a function of time by the following equation, yielding a characteristic time, τ, for the process.

$$X(t) = 1 - \exp(-t/\tau) \quad (6)$$

where $X(t)$ is the water uptake divided by equilibrium water uptake;

$$X(t) = \Delta w(t)/\Delta w_{final} \quad (7)$$

3. Results and discussion

Water sorption isobars and isotherms for Z02 powder, pellets, and coating samples are shown in Fig. 3 (a) and (b). Mitsubishi Plastics creates pellets and coatings from Z02 using a proprietary method that includes a silicon dioxide-based binder. The binder does not influence the isotherm shape. However, the water uptake per gram of dry adsorbent is lower for the pellets and coating in comparison to the pure Z02 powder due to the weight of binder in the adsorbent and, potentially, pore blockage. As shown in Fig. 3, the decrease in equilibrium water uptake for the Z02 pellets and coating samples was 9% and 13%, respectively, relative to the Z02 powder. This suggests that the Z02 coating contains a greater amount of binder by weight or the binder has impeded access to some zeolite powder grains or pores. The solution formulation in which the Z02 is suspended for dip coating is likely different than the one used for pelletizing.

For comparison, Calabrese et al.'s recent study of SAPO-34 coatings containing a polymer binder also used the difference in maximum water adsorption measured in isobars of coatings relative to pure zeolite samples to determine the percentage of active SAPO-34 content in the coatings, e.g. 96% of the SAPO-34 content was active for coatings containing 10 wt% binder [17].

Table 1
Adsorber bed specifications and operating conditions.

HEX (L,W,H)	35.2 cm × 3.8 cm × 30.5 cm	Cycle times	5, 10, 20, 30 min
Fin spacing	2.54 mm (10 fpi)	$T_{desorption}$	75, 80, 90 °C
Surface area	2.8 m^2	$T_{adsorption}$	20, 30, 40 °C
HEX weight	2.51 ± 0.03 kg	$T_{condenser}$	20, 30, 40 °C
Z02 coating	0.80 kg per HEX	$T_{evaporator}$	5, 10, 15 °C
Z02 pellets	1.97 kg per HEX		

The adsorption branches of eight Z02 pellet isotherms (5–80 °C, 285 data points) were used to generate the isosters that were fitted to determine the heat of adsorption as a function of water content, see Fig. 4. The isosteric heat of adsorption for the pellets for water content less than 0.3 g/g was −61 kJ/mol (−3400 kJ/kg). This is in agreement with isosteric heats of adsorption determined by Kayal et al. [19], and slightly greater than the values reported by Teo et al. [20]. Kakiuchi et al. reported a similar differential heat of adsorption for Z02, 58.3 kJ/mol at 298 K [1].

The nitrogen adsorption isotherms of the Z02 pellets and coating are compared in Fig. 5 (a), and shown separately in Fig. 5 (b) and (c) with the y-axis scales adjusted to better show the hysteresis in the desorption curves. The steep initial region ($< 0.15 P/P_0$) of the Z02 pellet nitrogen adsorption corresponds to the filling of micropores. The curve shape (Type IV, H4), particularly the hysteresis in the desorption branch of

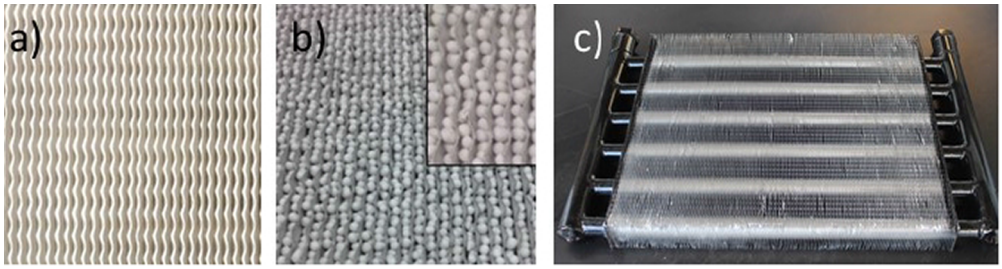

Fig. 2. (a) Heat exchanger (HEX) fins coated with Z02, (b) HEX fins packed with Z02 pellets, (c) empty sorber bed HEX.

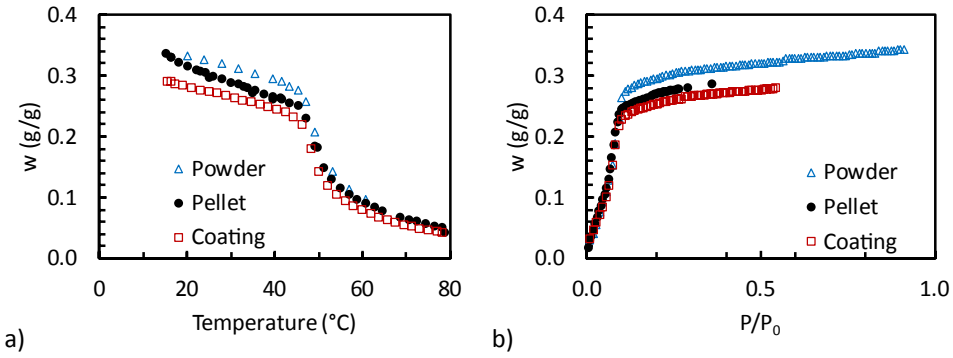

Fig. 3. Comparison of water vapor sorption of AQSOA FAM-Z02 powder, pellets (~2 mm diameter) and coating (a) isobars at 12 mbar and (b) isotherms at 35 °C.

the isotherm at higher partial pressure indicates that the material also has slit-like mesopores. The pore volume of the Z02 pellets calculated from the nitrogen adsorption was 0.3 cc/g (P/P_0 0.975, pores with radius < 38 nm). In contrast, multiple nitrogen adsorption isotherm runs on three samples (from 0.1 g to 0.7 g) of the Z02 coating yielded isotherms with low uptake at saturation pressure in all cases, 0.001–0.003 cc/g (P/P_0 0.975, pores with radius < 42 nm (Fig. 5a, c). The results suggest that the binder on the surface of the Z02 particles in the coating impedes the access of nitrogen molecules to the silicoaluminophosphate micropores.

FAM-Z02 has a chabazite (CHA) cage structure that water molecules enter through 0.38 nm windows [1]. Nitrogen molecules have a larger kinetic diameter (0.363 nm) than water molecules (0.265 nm), therefore it is possible to create a coating where water is adsorbed (Fig. 3a) and nitrogen is not adsorbed (Fig. 5c). A narrowing of the pore windows at the surface of zeolite by less than 0.02 nm could produce this effect. In this case, the results suggest that the surface coverage of binder on the sorbent grains is greater in the coating compared to the pellets.

As shown in Fig. 6, in lab-scale sorption chiller tests, the Z02 coated HEX had greater volumetric and mass specific cooling powers than the Z02 pellet filled HEX. This was in part due to the thermal contact resistance at the interface between the pellets and the HEX, which impedes heat transfer. Rouhani et al. measured the thermal conductivity of a packed bed of the Z02 pellets as 0.2 W $m^{-1}{\cdot}K^{-1}$, and determined that when a monolayer of pellets was pressed between metal plates under contact pressure of 0.7 kPa thermal contact resistance was 67% of the overall thermal resistance [21]. The pellets were tightly packed in the HEX and in contact with both sides of each fin (0.2 mm fin thickness, 2.54 mm fin spacing), however a relatively small portion of the pellets had both top and bottom contact points. The heat transfer surface/adsorbent mass ratios, S/m, for the pellet and coating sorber beds were 1.5 and 3.6 m^2/kg, respectively.

Sapienza et al. examined the effect of grain size and by large temperature jump, calculated VSCP for 80% of equilibrium water uptake, assuming a fixed dead volume, and found cooling power peaked at ~120 kW/m^3 for grain sizes between 1.1 and 1.6 mm, and declined sharply for larger grain sizes [22]. The pellet size available for the present study, average 1.9 mm, is considered to be a performance limiting factor, i.e. an increase in SCP and VSCP would be expected if the pellets were crushed into smaller, irregularly-shaped loose grains.

The Z02 coated HEX had an SCP of 456 W/kg (90 kW/m^3) and a COP of 0.27 for 10 min cycles. For 30 min cycles with the Z02 coated HEX, the uptake rate was 0.04–0.05 g/100 g·s during the first 4 min of sorption while 96% of sorption capacity was achieved in 10 min. Dawoud reported a sorption rate of 0.06 g/100 g·s for small samples of 0.3 mm Z02 coatings, and much lower uptake rates for HEX coated with 1.5 kg of sorbent (57% uptake capacity in 10 min) [10].

For comparison, the SAPO-34 directly crystallized on an aluminium fiber flat tube HEX tested by Wittstadt et al. had a SCP of 478 W/kg and VSCP for the adsorber bed (without header) of 190 kW/m^3 when tested with 12, 32, 32 and 90 °C operating conditions [14]. The difference in VSCP between the aforementioned study and the results presented here is consistent with the greater sorbent loading possible in the fiber flat tube HEX (0.39 kg/L compared to 0.20 kg/L), although there are other differences between the systems (single module versus 2 bed). Even greater VSCP of 286 kW/m^3 by adsorber volume was achieved by the 3-bed sorption system with hybrid sorber beds combining a Z02 coating with loose grain silica gel for tests at 15, 28, 28, and 90 °C, which also had a greater SCP, 508 W/kg [12]. Sorption chiller tests on a small coated HEX (0.08 kg sorbent) by Freni et al. achieved 93 kW/m^3 and 675 W/kg [9].

The evaporator inlet and outlet temperatures were used to determine the total heat transfer measured at the evaporator per cycle, see Eq. (2). The system performance metrics (SCP and COP) are shown in Fig. 6 for Z02 coated beds operated with 5, 16 and 30 min cycles and evaporator, condenser, adsorption and desorption temperatures of 15, 30, 30 and 90 °C, respectively. The reported SCP values are the average calculated from measurements of 4 to 7 consecutive cycles of the

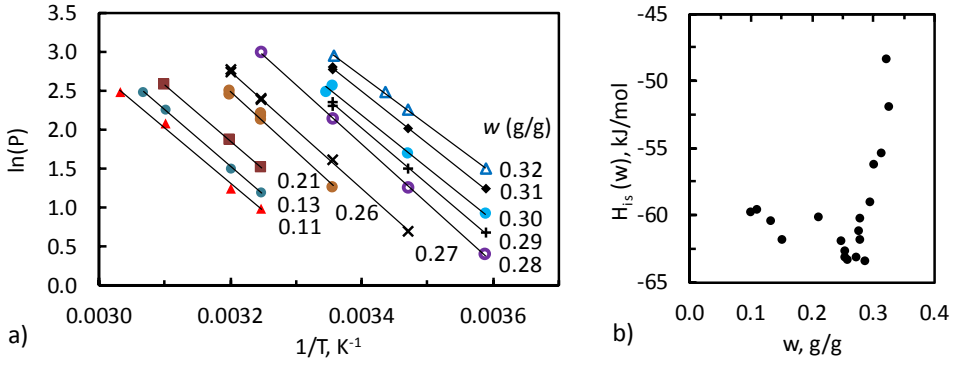

Fig. 4. (a) Water vapor sorption isosters for AQSOA-Z02 pellets, and (b) the isosteric heat of adsorption of AQSOA FAM-Z02 pellets as a function of water content.

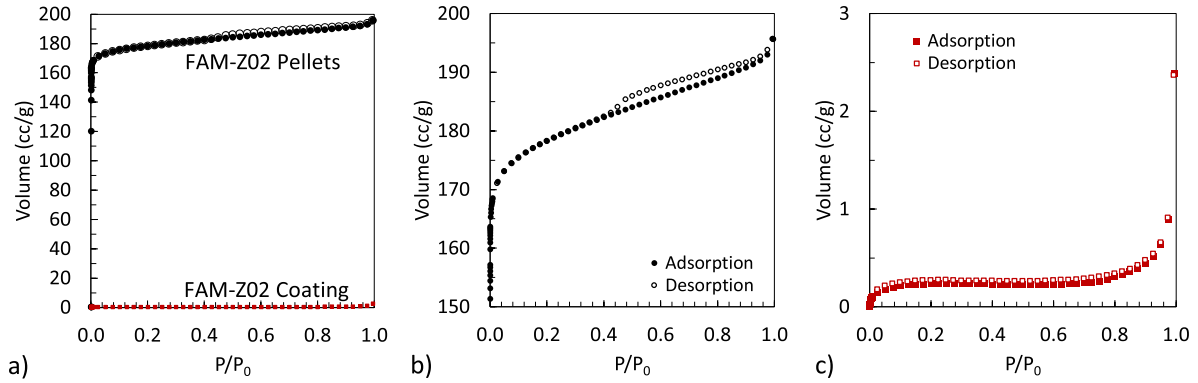

Fig. 5. (a) Nitrogen adsorption isotherms for AQSOA-Z02 pellets and coating, (b) isotherm detail for the pellets, and (c) isotherm detail for the coating.

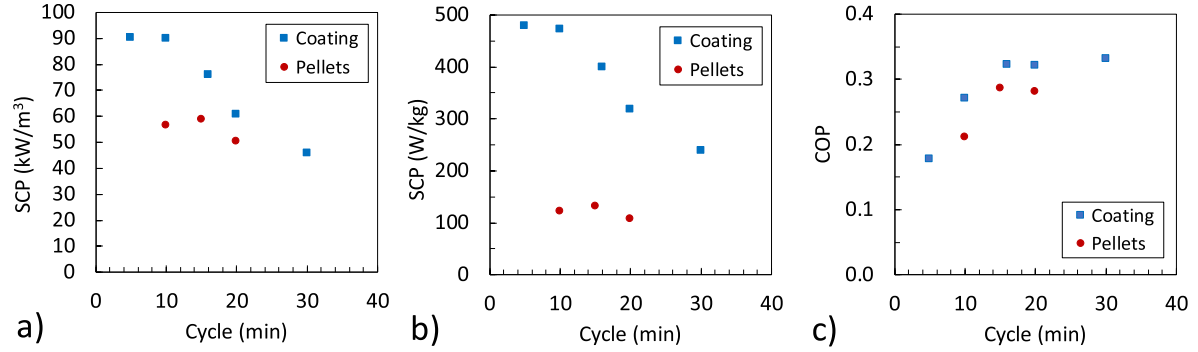

Fig. 6. Performance of sorption chiller for Z02 coating and pellet; (a) VSCP by HEX volume, (b) SCP by sorbent weight, and (c) COP. Operating conditions: $T_{evaporator}$ = 15 °C, $T_{condenser}$ = $T_{adsorption}$ = 30 °C, and $T_{desorption}$ = 90 °C. SCP and COP measurement uncertainty was 7.5% and the standard deviation for cycle to cycle SCP measurements ranged from 0.5 to 3%.

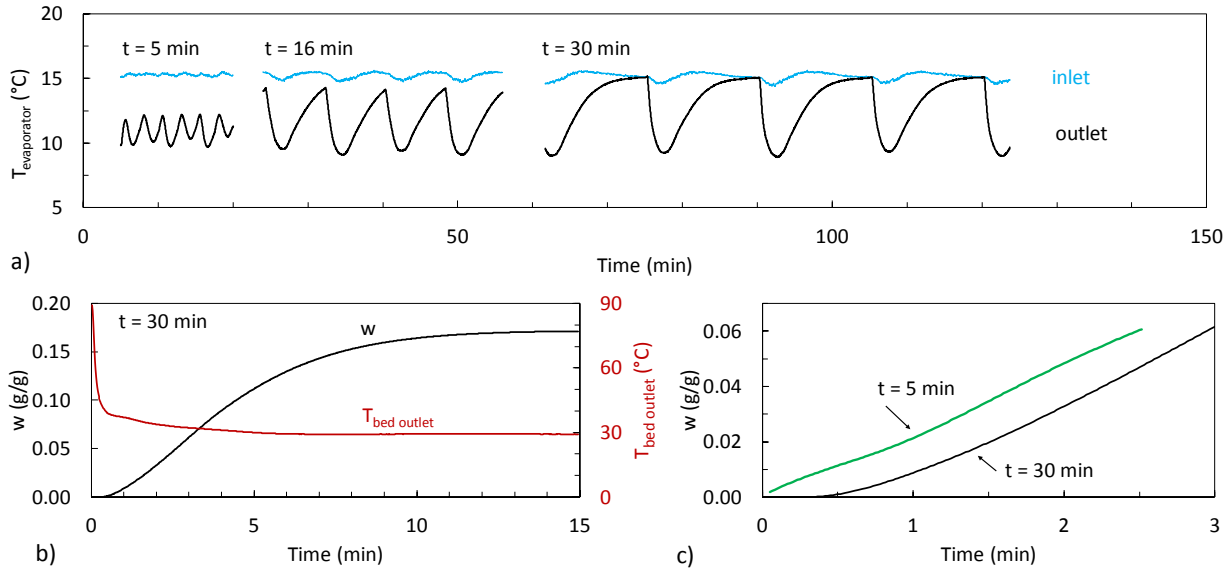

Fig. 7. (a) The inlet and outlet temperatures of the evaporator for different cycle times. The sorption as a function of time calculated from the cooling power delivered by the evaporator for (b) the 30-minute cycles, and (c) the first minutes of sorption for short and long cycles. Note: The initial uptake rate is under represented for the equilibrium (30 min) cycles as the thermal inertia of the evaporator was not included in the calculation.

system. The cooling power can be used to calculate the evaporation rate and, consequently, the uptake rate of the active adsorber bed.

The inlet and outlet temperatures of the heat transfer fluid (water) to the evaporator are shown for different cycle times in Fig. 7 (a). Fig. 7 (b) shows the cumulative uptake as a function of time for a 15 min half cycle including the initial brief transition period during which the temperature of the bed decreases from the desorption temperature (the outlet temperature of the 30 °C bed cooling loop is shown in red). No evaporation occurs until after the vapor pressure in the adsorber decreases, triggering the opening of the valve between the adsorber and evaporator (~20 s for the cycle shown).

For 30 min cycles, the calculated initial uptake rate is underestimated as the delivered cooling power used for the calculation does not include the evaporation required to rapidly cool the evaporator

(~4.5 kg of copper) from 15 °C to 9 °C. As shown, the temperature fluctuation of the evaporator was much lower for shorter cycles, and the impact of the thermal inertia of the evaporator on the adsorbent water uptake calculation was less significant, Fig. 7 (a) and (c). Neglecting the initial 150 s of the half cycle, correlations of the dimensionless uptake as a function of time, as per Eq. (6), of six half cycles yielded an average characteristic time of 194 ± 2 s for the system operating with Z02 coating (800 g per HEX).

4. Summary

The performance of the lab-scale sorption chiller was comparable to the expected potential of Z02 coatings based on previous kinetic studies of small samples and small coated heat exchangers. For the operating conditions tested, Z02 coated sorber beds the highest cooling power observed was 456 W/kg (90 kW/m^3) for 10 min cycles for which system the COP was 0.27. Correlations of water uptake rates from tests with longer cycle times yielded a characteristic time, τ, of 194 ± 2 s.

CRediT authorship contribution statement

C. McCague: Writing - original draft, Investigation, Conceptualization. **W. Huttema:** Investigation. **A. Fradin:** Investigation. **M. Bahrami:** Supervision, Funding acquisition, Writing - review & editing.

Declaration of Competing Interest

The authors declare that they have no known competing financial interests or personal relationships that could have appeared to influence the work reported in this paper.

Acknowledgements

The authors gratefully acknowledge the financial support of the Natural Sciences and Engineering Research Council of Canada (NSERC) through the Automotive Partnership Canada Grant No. APCPJ 401826-10.

Appendix A

The heat transfer rate in the evaporator is calculated from the measured flowrate and inlet to outlet ΔT of the thermal fluid (water) as follows

$$\dot{Q}_{evap} = \dot{m} c_p (T_{\text{in}} - T_{\text{out}})$$

and the instrumental uncertainty is

$$\frac{\delta \dot{Q}_{evap}}{\dot{Q}_{evap}} = \sqrt{\left(\frac{\delta \dot{m}}{\dot{m}}\right)^2 + \left(\frac{\delta c_p}{c_p}\right)^2 + \left(\frac{\sqrt{\delta T_{in}^2 + \delta T_{out}^2}}{(T_{\text{in}} - T_{\text{out}})}\right)^2} = \sqrt{(0.005)^2 + (0.0007)^2 + (0.07)^2}$$

The uncertainty of the calculated SCP (Eq. (4)) is therefore

$$\frac{\delta SCP}{SCP} \times 100 = \sqrt{\left(\frac{\delta Q_{evap}}{Q_{evap}}\right)^2 + \left(\frac{\delta m_{ads}}{m_{ads}}\right)^2 + \left(\frac{\delta t_{cycle}}{t_{cycle}}\right)^2} \times 100 = \sqrt{(0.07)^2 + (20/800)^2 + (1/300)^2} \times 100 = 7.5\%$$

where the relatively large uncertainty (± 20 g) in the adsorbent mass, m_{ads}, is due to differences in the weights of the empty and coated heat exchangers reported by Mitsubishi Chemical Corporation and the values measured in our laboratory. Each reported SCP is the average of 4 to 7 consecutive cycles, and standard deviations for the cycle to cycle variations for the sorbents and cycle times tested ranged from 0.5 to 3% of the reported value.

$$\frac{\delta COP}{COP} \times 100 = \sqrt{\left(\frac{\delta Q_{evap}}{Q_{evap}}\right)^2 + \left(\frac{\delta Q_{desorp}}{Q_{desorp}}\right)^2} \times 100 = \sqrt{(0.07)^2 + (0.1)^2}$$

The greater uncertainty in the T type thermocouples used to monitor the inlet and outlet temperature of the thermal fluid (water) used for desorption at 90 °C.

Appendix B. Supplementary material

Supplementary data to this article can be found online at https://doi.org/10.1016/j.applthermaleng.2020.115219.

References

[1] H. Kakiuchi, M. Iwade, S. Shimooka, K. Ooshima, M. Yamazaki, T. Takewaki, Novel zeolite adsorbents and their application for AHP and desiccant system, in: Proc. IEA Annex-17 Meeting, Beijing, China, 2005.
[2] A. Freni, G. Maggio, A. Sapienza, A. Frazzica, G. Restuccia, S. Vasta, Comparative analysis of promising adsorbent/adsorbate pairs for adsorptive heat pumping, air conditioning and refrigeration, Appl. Therm. Eng. 104 (2016) 85–95, https://doi.org/10.1016/j.applthermaleng.2016.05.036.
[3] I.S. Girnik, Yu.I. Aristov, Dynamics of water vapour adsorption by a monolayer of loose AQSOA™-FAM-Z02 grains: Indication of inseparably coupled heat and mass transfer, Energy 114 (2016) 767–773, https://doi.org/10.1016/j.energy.2016.08.056.
[4] I.S. Girnik, Yu.I. Aristov, Dynamic optimization of adsorptive chillers: The "AQSOA™-FAM-Z02 – Water" working pair, Energy 106 (2016) 13–22, https://doi.org/10.1016/j.energy.2016.03.036.
[5] S. Santamaria, A. Sapienza, A. Frazzica, A. Freni, I.S. Girnik, Yu.I. Aristov, Water adsorption dynamics on representative pieces of real adsorbers for adsorptive chillers, Appl. Energy 134 (2014) 11–19, https://doi.org/10.1016/j.apenergy.2014.07.053.
[6] J. Ammann, B. Michel, P.W. Ruch, Characterization of transport limitations in SAPO-34 adsorbent coatings for adsorption heat pumps, Int. J. Heat Mass Transf. 129 (2019) 18–27, https://doi.org/10.1016/j.ijheatmasstransfer.2018.09.053.
[7] J. Ammann, B. Michel, A.R. Studart, P.W. Ruch, Sorption rate enhancement in SAPO-34 zeolite by directed mass transfer channels, Int. J. Heat Mass Transf. 130 (2019) 25–32, https://doi.org/10.1016/j.ijheatmasstransfer.2018.10.065.
[8] J. Ammann, P. Ruch, B. Michel, A.R. Studart, Quantification of heat and mass transport limitations in adsorption heat exchangers: application to the silica gel/water working pair, Int. J. Heat Mass Transf. 123 (2018) 331–341, https://doi.org/10.1016/j.ijheatmasstransfer.2018.02.076.
[9] S. Mitra, et al., Study on the influence of adsorbent particle size and heat exchanger aspect ratio on dynamic adsorption characteristics, Appl. Therm. Eng. 133 (2018) 764–773.
[10] A. Freni, A. Frazzica, B. Dawoud, S. Chmielewski, L. Calabrese, L. Bonaccorsi, Adsorbent coatings for heat pumping applications: Verification of hydrothermal and mechanical stabilities, Appl. Therm. Eng. 50 (2013) 1658–1663, https://doi.org/10.1016/j.applthermaleng.2011.07.010.

[11] A. Freni, L. Bonaccorsi, L. Calabrese, A. Caprì, A. Frazzica, A. Sapienza, SAPO-34 coated adsorbent heat exchanger for adsorption chillers, Appl. Therm. Eng. 82 (2015) 1–7, https://doi.org/10.1016/j.applthermaleng.2015.02.052.
[12] A. Sapienza, G. Gullì, L. Calabrese, V. Palomba, A. Frazzica, V. Brancato, D. La Rosa, S. Vasta, A. Freni, L. Bonaccorsi, G. Cacciola, An innovative adsorptive chiller prototype based on 3 hybrid coated/granular adsorbers, Appl. Energy 179 (2016) 929–938, https://doi.org/10.1016/j.apenergy.2016.07.056.
[13] B. Dawoud, Water vapor adsorption kinetics on small and full scale zeolite coated adsorbers; A comparison, Appl. Therm. Eng. 50 (2013) 1645–1651, https://doi.org/10.1016/j.applthermaleng.2011.07.013.
[14] U. Wittstadt, G. Füldner, E. Laurenz, A. Warlo, A. Große, R. Herrmann, L. Schnabel, W. Mittelbach, A novel adsorption module with fiber heat exchangers: Performance analysis based on driving temperature differences, Renewable Energy 110 (2017) 154–161, https://doi.org/10.1016/j.renene.2016.08.061.
[15] L. Calabrese, L. Bonaccorsi, P. Bruzzaniti, E. Proverbio, A. Freni, SAPO-34 based zeolite coatings for adsorption heat pumps, Energy 187 (2019) 115981, , https://doi.org/10.1016/j.energy.2019.115981.
[16] A. Sharafian, S.M. Nemati Mehr, P.C. Thimmaiah, W. Huttema, M. Bahrami, Effects of adsorbent mass and number of adsorber beds on the performance of a waste-heat driven adsorption cooling system for vehicle air conditioning applications, Energy 112 (2016) 481–493, https://doi.org/10.1016/j.energy.2016.06.099.
[17] P.C. Thimmaiah, A. Sharafian, W. Huttema, C. McCague, M. Bahrami, Effects of capillary-assisted tubes with different fin geometries on the performance of a low-operating pressure evaporator for adsorption cooling systems, Appl. Energy 112 (2016) 481–493, https://doi.org/10.1016/j.energy.2016.06.099.
[18] P.C. Thimmaiah, A. Sharafian, M. Rouhani, W. Huttema, M. Bahrami, Evaluation of low-pressure flooded evaporator performance for adsorption chillers, Energy 122 (2017) 144–158, https://doi.org/10.1016/j.energy.2017.01.085.
[19] S. Kayal, S. Baichuan, B.B. Saha, Adsorption characteristics of AQSOA zeolites and water for adsorption chillers, Int. J. Heat Mass Transf. 92 (2016) 1120–1127, https://doi.org/10.1016/j.ijheatmasstransfer.2015.09.060.
[20] H.W.B. Teo, A. Chakraborty, W. Fan, Improved adsorption characteristics data for AQSOA types zeolites and water systems under static and dynamic conditions, Microporous Mesoporous Mater. 242 (2017) 109–117, https://doi.org/10.1016/j.micromeso.2017.01.015.
[21] M. Rouhani, W. Huttema, M. Bahrami, Effective thermal conductivity of packed bed adsorbers: Part 1 – Experimental study, Int. J. Heat Mass Transf. 123 (2018) 1204–1211, https://doi.org/10.1016/j.ijheatmasstransfer.2018.01.142.
[22] A. Sapienza, S. Santamaria, A. Frazzica, A. Freni, Yu.I. Aristov, Dynamic study of adsorbers by a new gravimetric version of the Large Temperature Jump method, Appl. Energy 113 (2014) 1244–1251, https://doi.org/10.1016/j.apenergy.2013.09.005.